Chapter 43

NUMERICAL PREDICTION ON TYPHOON TIDE IN TOKYO BAY

Takeshi Ito, Mikio Hino
Central Research Institute of Electric Power Industry
Komae-cho, Kitatama-gun, Tokyo, Japan

Jiro Watanabe, Kazuko Hino
Mitsubishi Atomic Power Industries Inc.
Ōtemachi, Chiyoda-ku, Tokyo, Japan

ABSTRACT

The paper discusses firstly mathematical problems on the numerical calculation of storm surges. The partial differential equations of motion adopted here take into account the Coriolis force and the non-linear terms such as the inertial terms and a quadratic form of bottom friction. As a result, special care must be taken in order to obtain stable forms of finite-difference equations. It is shown that inadequate forms accumulate errors to cause divergence of the step by step calculations. A set of stable forms of the finite-difference equations of motion and continuity has been derived.

Sometimes, it is convenient to divide the numerical integration region into two or more sub-regions, the mesh-dimensions of which are not equal. A method is described to calculate both regions by one procedure.

Japan coasts were frequently damaged by severe storm surges (Typhoon Tides). To protect the metropolitan area from storm surges, a proposal has been made to construct a dike across Tokyo Bay. A numerical calculation has been made by means of IBM 7090 to estimate for several opening width of the proposed dike its effects on the reduction of surges. Interactions between daily tides (astronomical tide) and surges are also discussed.

INTRODUCTION

A rapid development of the industrial activities is now going on in the urban districts of Japan, especially in the metropolitan area around Tokyo Bay. The expected increase of the urbanization and industrial activities will ask for improvement of traffic conditions and for remodeling of the metropolitan centre and its through ways. From this point of view, a proposal has been made by the Council for Industry Planning to construct a dike (of length about 18 km) across the central part of Tokyo Bay, which connects the over-crowded area of Tokyo, Kawasaki and Yokohama on the west side to the developing industrial area on the other side of the bay.

On the other hand, Japanese coasts have been frequently damaged by severe storm surges (Typhoon tides or TAKASHIO in Japanese). To protect the metropolitan area from storm surges, the proposed dike is expected to be also effective, probably reducing the typhoon water level. Thus, it would seem that there will be a chance of killing two birds with one stone

Here, care must be taken in that the dike is not situated on the entrance of the bay but on the central part. A check on the effectiveness of the two positions for reduction of storm surges has already been made to conclude that the central position is superior to the other.

Two reports Miyazaki (1961), Unoki and Isozaki (1962) have been published on the numerical prediction of the typhoon tides and of the effectiveness of the proposed dike. A precise and comprehensive numerical calculation by means of IBM 7090 is presented in this paper. Numerical integrations in the earlier ones were limited within the bay (north region above Kurihama). Two openings for navigation, each of 500 m, were situated on east and west ends of the dike. The openings have been removed in our calculation to the centre of the dike according to the recommendation by P. Ph. Jansen and J.J. Dronkers (1962). In order to give more precise boundary conditions the region of numerical integration has been extended, about nine times in area, to the outer part of the bay into the Pacific Ocean where the depth is a thousand meter or more.

In these calculations, great difficulties are encounted because we can no more neglect as usually done the non-linear inertial terms at the opening. Further computational problems are experienced by introduction of the Coriolis force and a quadratic form of bottom friction which in the earlier computations is approximated by a linear form. These will be discussed as the stability problem of the finite-difference equations.

Sometimes, it is convenient to divide the numerical integration region into two or more sub-regions, the mesh dimensions of which are not equal. In this computation, the integration area has been extended from Tokyo Bay(about 1000 km^2) to the outer region (about 9000 km^2). A method is described to calculate the two regions by one procedure.

MATHEMATICAL PROBLEMS

FUNDAMENTAL EQUATIONS AND BOUNDARY CONDITIONS

The hydrodynamic equations of motion and continuity in two-dimension are represented, with use of the volume of water transported in unit time across vertical section of unit width between the free surface and the bottom, by

$$\frac{\partial M}{\partial t}+\frac{M}{(h+\zeta)}\frac{\partial M}{\partial x}+\frac{N}{(h+\zeta)}\frac{\partial M}{\partial y}=-g(h+\zeta)\frac{\partial(\zeta-\zeta_o)}{\partial x}+fN-\frac{\tau_b^{(x)}}{\rho_W}+\frac{\tau_s^{(x)}}{\rho_W} \tag{1}$$

$$\frac{\partial N}{\partial t}+\frac{M}{(h+\zeta)}\frac{\partial N}{\partial x}+\frac{N}{(h+\zeta)}\frac{\partial N}{\partial y}=-g(h+\zeta)\frac{\partial(\zeta-\zeta_o)}{\partial y}-fM-\frac{\tau_b^{(y)}}{\rho_W}+\frac{\tau_s^{(y)}}{\rho_W} \tag{2}$$

$$\frac{\partial \zeta}{\partial t}=-\left(\frac{\partial M}{\partial x}+\frac{\partial N}{\partial y}\right) \tag{3}$$

where t = time coordinate
x, y = coordinate system (x = east, y = north direction)
U, V = velocity components taken as means in vertical line, in x and y direction respectively
$M = UH$
$N = VH$
$H = h + \zeta$
h = mean water depth
ζ = elevation above mean sea-level
$\zeta_0 = \Delta p/\rho_w g$
Δp = atmospheric pressure drop
$f = 2\omega \sin\varphi$, Coriolis parameter
ω = angular speed of the rotation of the earth
φ = latitude
g = acceleration of gravity
ρ_w = specific weight of water

External forces, τ_s (wind stress), τ_b (bottom friction) and ζ_0 are given by

$$\vec{\tau}_s = \rho_a \gamma^2 \, |W| W \qquad (\rho_a \gamma^2 = 32 \times 10^{-6}) \tag{4}$$

$$\vec{\tau}_b = \rho_w \gamma^2 \, |V| V - \kappa_s \vec{\tau}_s \tag{5}$$

$$\zeta_0 = \frac{a}{\rho_w g} \left\{ 1 + \left(\frac{r}{r_0}\right)^2 \right\}^{-\frac{1}{2}} \tag{6}$$

where the wind velocity W is represented by eqs. (7) and (8)

$$W_y = C_1 U_x \exp\left(-\frac{r\pi}{5 \times 10^7}\right) - \frac{C_2 f}{2} \left[-1 + \sqrt{1 + \frac{4a}{\rho_a f^2} \cdot \frac{1}{r_0^2 \left\{1 + \left(\frac{r}{r_0}\right)^2\right\}^{\frac{3}{2}}}} \right] \tag{7}$$
$$(0.500x + 0.866y)$$

$$W_y = C_1 U_y \exp\left(-\frac{r\pi}{5 \times 10^7}\right) - \frac{C_2 f}{2} \left[-1 + \sqrt{1 + \frac{4a}{\rho_a f^2} \cdot \frac{1}{r_0^2 \left\{1 + \left(\frac{r}{r_0}\right)^2\right\}^{\frac{3}{2}}}} \right] \tag{8}$$
$$(0.866x - 0.500y)$$

r = distance from the centre of a tropical cyclone (typhoon)
a, r_0 = constants referred to the intensity and range of typhoon, respectively
U_x, U_y = speed of center of typhoon
C_1, C_2 = constants
$V = U + iV$

Equation (6) is an empirical formula by Fujita giving atmospheric pressure drop due to cyclone. Eqs. (7) and (8) are derived from eq. (6).

Boundary conditions are given as follows: On natural coastal lines,

there exists no mass transport, M = N = 0. Also the mass transport perpendicular to the axis of the dike is zero. Elevations of water level on boundaries in the Pacific Ocean are given equal to the sum of the water-level rises due to the atmospheric pressure drop (ζ_0) and the astronomical or daily tides (ζ_*); $\zeta = \zeta_0 + \zeta_*$.

STABILITY OF FINITE-DIFFERENCE EQUATION

To carry out the numerical integration, the hydrodynamic equations are to be reduced to the finite difference forms. It is well known that for numerical stability of successive calculations a relationship between the space-difference $\triangle s$ and the time-difference $\triangle t$ should be satisfied such as

$$\frac{\Delta s}{\Delta t} \geq \sqrt{2gh_{max}} \tag{9}$$

This is the so-called "Courant-Friedrichs-Lewy criterion." One should use such small time-steps that the above condition is well fulfilled.

Besides of this, a complicated problem is provoked when non-linear terms such as a quadratic form of bottom friction and the inertial terms are taken into account.

One way to investigate the numerical stability is an numerical experiments to decide what forms of the innumerable finite-difference versions are stable. Shuman (1962), with a numerical experience of one-dimensional model, showed that the semi-momentum and the filtered factor forms exhibited no significant instability.

However, in our case, the change of the inertial term, especially at the opening, is so local that neither of the finite-difference forms recommended by Shuman was available.

Therefore, the stability problems were investigated as described in the followings

In order to clarify the logic, we will discuss the stable finite-difference forms of three elementary types of partial differential equations.

a) Firstly, the simple differential equation (10) will be treated.

$$\frac{dM}{dt} = aM + f(t) \tag{10}$$

Denoting $(M)_{t=n\Delta t}$ by M^n, equation (10) can be reduced to equation (11),

$$(M^{n+1} - M^{n-1})/2\triangle t = aM^n + f(n) \tag{11}$$

A vector defined by $X^n = (M^n, M^{n-1})$ is transformed into a vector $X^{n+1} = (M^{n+1}, M^n)$ through a linear operator R

$$R = \begin{pmatrix} 2a\triangle t & 1 \\ 1 & 0 \end{pmatrix} \tag{12}$$

The eigenvalue λ of the operator R is given by

$$\lambda = a\triangle t \pm \sqrt{a^2\triangle t^2 + 1} \tag{13}$$

For $a < 0$, λ becomes $|\lambda| > 1$. Thus, the finite-difference equation (11) is always unstable for $a < 0$. A stable finite-difference form is obtained

by replacing the term aM^n in eq.(11) by $a(M^{n+1}+M^{n-1})/2$ as demonstrated in the next section.

b) Next, the partial differential equations which include the Coriolis force and the bottom friction of quadratic form will be treated,

$$\frac{\partial M}{\partial t} = fN - eM\sqrt{M^2+N^2} + C_1 \tag{14}$$

$$\frac{\partial N}{\partial t} = -fM - eN\sqrt{M^2+N^2} + C_2 \ . \tag{15}$$

$$(M = M_o , N = N_o \quad at \quad t = t_o)$$

It will easily be seen from the result of a)that eqs. (14) and (15) should not be reduced as

$$\frac{M^{n+1}-M^{n-1}}{2\triangle t} = fN^n - \{ e\sqrt{(M^n)^2+(N^n)^2}\ \}M^n + C_1 \ . \tag{16}$$

However, the following forms, eqs. (17) and (18) may be shown to be stable,

$$\frac{M^{n+1}-M^{n-1}}{2\Delta t} = fN^n - \frac{e}{2}(M^{n+1}+M^{n-1})\sqrt{(M^n)^2+(N^n)^2} + C_1 \tag{17}$$

$$\frac{N^{n+1}-N^{n-1}}{2\triangle t} = -fM^n - \frac{e}{2}(N^{n+1}+N^{n-1})\sqrt{(M^n)^2+(N^n)^2} + C_2 \ . \tag{18}$$

Here, transformations as follows are introduced,

$$\left.\begin{aligned} \alpha &= \frac{1-e\Delta t\sqrt{(M^n)^2+(N^n)^2}}{1+e\Delta t\sqrt{(M^n)^2+(N^n)^2}} \ ; \ \beta = \frac{2f\Delta t}{1+e\Delta t\sqrt{(M^n)^2+(N^n)^2}} \\ \gamma_1 &= \frac{2C_1\Delta t}{1+e\Delta t\sqrt{(M^n)^2+(N^n)^2}} \ ; \ \gamma_2 = \frac{2C_2\Delta t}{1+e\Delta t\sqrt{(M^n)^2+(N^n)^2}} \end{aligned}\right\} \tag{19}$$

Considering the fact that the divergence of step-by-step calculations due to instability grows within a few decade of steps the factors α, β, γ_1, and γ_2 may be treated as constants.
Equations (17) and (18) are represented as

$$M^{n+1} = \alpha M^{n-1} + \beta M^n + \gamma_1 \tag{20}$$

$$N^{n+1} = \alpha N^{n-1} - \beta M^n + \gamma_2 \tag{21}$$

Furthermore, they can be rewritten using the matrix expression,

$$X_1 = \begin{bmatrix} M^{1-1} \\ N^{1-1} \\ M^1 \\ N^1 \end{bmatrix} \ , \ Y = \begin{bmatrix} 0 \\ 0 \\ \gamma_1 \\ \gamma_2 \end{bmatrix} \ ; \ R = \begin{bmatrix} 0 & 0 & 1 & 0 \\ 0 & 0 & 0 & 1 \\ \alpha & 0 & 0 & \beta \\ 0 & \alpha & -\beta & 0 \end{bmatrix} \tag{22}$$

$$X_{n+1} = RX_n + Y \ . \tag{23}$$

By repetition, eq. (23) reduces to

$$X_{n+1} = R^n X_1 + (R^{n-1} + R^{n-2} + \cdots + R^2 + R + E)\,Y \tag{24}$$

where E means the unit matrix of four dimensions. Therefore, the stability condition for the finite difference equation is given such that the absolute values of all roots of secular equation (25)

$$|\lambda E - R| = (\lambda^2 - \alpha)^2 + \beta^2\lambda^2 = 0 \tag{25}$$

should be smaller than unity or at the most one of the roots may be equal to unity but it should not be double roots. Because $0<\beta \ll \alpha<1$, eigenvalues λ of the determinant R ($|\lambda|^2 = \alpha$) are smaller than unity. As a consequence, the finite-difference equations of the form eqs. (17) and (18) are shown to be stable.

c) Two finite difference versions of the inertial term abreviated as eq. (27) are considered,

$$\frac{\partial u}{\partial t} = -u\frac{\partial u}{\partial x} + f(t,x)\ (0<x<1,\ u(0)=u(1)=0) \tag{26}$$

$$\text{(I)}\quad \frac{u_i^{n+1}-u_i^n}{\Delta t} = -\overline{u_i^n}\,\frac{(u_{i+1}^n - u_{i-1}^n)}{2\Delta x} + f_i^n \tag{27}$$

$$\text{(II)}\quad \frac{u_i^{n+1}-u_i^n}{\Delta t} = -\overline{u_i^n}\,\frac{(u_{i+1}^n - u_i^n)}{\Delta x} + f_i^n \qquad (\overline{u_i^n} \le 0) \tag{28}$$

$$\frac{u_i^{n+1}-u_i^n}{\Delta t} = -\overline{u_i^n}\,\frac{(u_i^n - u_{i-1}^n)}{\Delta x} + f_i^n \qquad (\overline{u_i^n} \ge 0) \tag{29}$$

where suffix i refers to a mesh-point and n to a time-step

Let $r = -\overline{u_i^n}\,\Delta t/\Delta x$, $V_i = u_i^{n+1}$ and $u_i = u_i^n$. A (n-1)-dimensional vector $\vec{u} = (u_1, u_2, \cdots, u_{n-1})$ is transformed to a vector $\vec{V} = (v_1, v_2, \cdots, u_{n-1})$ through operators R_I (for eq. (27)), R_{II} (for eq. (28)) and R_{II}' (for eq. (29)),

$$\text{(I)}\quad R_I : v_i = u_i + \frac{r}{2}(u_{i+1} - u_{i-1})\ (i=1, 2, \cdots, N-1) \tag{30}$$

$$\text{(II)}\quad R_{II} : v_i = (1-r)u_i + ru_{i+1} \qquad (r>0) \tag{31}$$

$$R_{II}' : v_i = (1+r)u_i - ru_{i-1} \qquad (r<0) \tag{32}$$

where matrices are represented by

$$R_I = \begin{bmatrix} 1 & r/2 & & & 0 \\ -r/2 & 1 & r/2 & & \\ & -r/2 & 1 & r/2 & \\ & & \ddots & \ddots & \ddots \\ & & & -r/2 & 1 & r/2 \\ 0 & & & & r/2 & 1 \end{bmatrix} \tag{33}$$

$$R_{II} = \begin{bmatrix} 1-r & r & & & \\ 0 & 1-r & r & & \\ & 0 & 1-r & r & \\ & & \ddots & \ddots & \ddots \\ & & & 0 & 1-r & r \\ & & & & 0 & 1-r \end{bmatrix} \qquad R_{II}' = \begin{bmatrix} 1-r & 0 & & & \\ -r & 1-r & 0 & & \\ & -r & 1-r & 0 & \\ & & \ddots & \ddots & \ddots \\ & & & -r & 1-r & 0 \\ & & & & -r & 1-r \end{bmatrix} \tag{34}$$

Eigenvalues of the matrix R_I are sum of eigenvalues of the matrix $S = R_I - E$ and 1. While, the matrix S being skew-symmetric, eigenvalues are purely immaginary Therefore, the absolute value of eigenvalues of R_I is always greater than unity. The finite-difference of (27) cannot be stable.

Whereas, eigenvalues of R_{II} and R_{II}' are $(1 - r)$ $(r \geq 0)$ and $(1 + r)$ $(r \leq 0)$, respectively. Thus, eqs. (28) and (29) are numerically stable.

In fact, our earlier calculations showed that the finite-difference form of the bottom friction and the Coriolis force such as

$$\frac{M^{n+1} - M^{n-1}}{2\Delta t} = fN^n - \{ g \sqrt{(M^n)^2 + (N^n)^2} \} \cdot M^n + C$$

produced the divergence of step by step calculation. Also, the finite-difference forms of the inertial terms such as

$$-\frac{N_{J,k}^n}{(h+\zeta)} \quad \frac{N_{J,k+1}^n - N_{J,k-1}^n}{2\Delta s} \quad \text{or} \quad -\frac{N_{J,k}^{n+1} + N_{J,k}^n}{2(h+\zeta)} \cdot \frac{N_{J,k+1}^n - N_{J,k-1}^n}{2\Delta s}$$

were very unstable yielding the divergence of numerical solution

Finally, from the above mentioned discussions, a set of stable finite-difference equations is derived.

$$M_{J,k}^{n+2} = \frac{1}{[1 + \frac{c}{2} d(x,y) \sqrt{(M_{J,k}^n)^2 + (N_{J,k}^n)^2}]} [M_{J,k}^n - a(x,y) \{ \zeta_{J+1,k}^{n+1} - \zeta_{0\,J-1,k}^{n+1} - \zeta_{J-1,k}^{n+1} + \zeta_{0\,J+1,k}^{n+1} \} + bN_{J,k}^{n+1} - \frac{c}{2} \{ d(x,y) M_{J,k}^n \sqrt{(M_{J,k}^n)^2 + (N_{J,k}^n)^2} - 3\tau_{s\,J,k}^{(x)\,n} \} - I_{11} - I_{12}] \tag{35}$$

where

$$I_{11} \begin{cases} = f(x,y) M_{J,k}^n \{ M_{J,k}^n - M_{J-1,k}^n \} & (M_{J,k}^n \geq 0) \\ = f(x,y) M_{J,k}^n \{ M_{J+1,k}^n - M_{J,k}^n \} & (M_{J,k}^n < 0) \end{cases} \tag{35a}$$

$$I_{12} \begin{cases} = f(x,y) N_{J,k}^n \{ M_{J,k}^n - M_{J,k-1}^n \} & (M_{J,k}^n \geq 0) \\ = f(x,y) N_{J,k}^n \{ M_{J,k+1}^n - M_{J,k}^n \} & (N_{J,k}^n < 0) \end{cases} \tag{35b}$$

$$N_{J,k}^{n+2} = \frac{1}{[1 + \frac{c}{2} d(x,y) \sqrt{(M_{J,k}^n)^2 + (N_{J,k}^n)^2}]} [N_{J,k}^n - a(x,y) \{ \zeta_{J,k+1}^{n+1} - \zeta_{0J,k-1}^{n+1} - \zeta_{J,k-1}^{n+1} + \zeta_{0J,k-1}^{n+1} \} - bM_{J,k}^{n+1} - \frac{c}{2} \{ d(x,y) N_{J,k}^n \sqrt{(M_{J,k}^n)^2 + (N_{J,k}^n)^2} - 3\tau_{J,k}^{s(x)} \} - I_{21} - I_{22}] \tag{36}$$

where

$$I_{21} \begin{cases} = f(x,y) M_{J,k}^n \{ N_{J,k}^n - N_{J-1,k}^n \} & (M_{J,k}^n \geq 0) \\ = f(x,y) M_{J,k}^n \{ N_{J+1,k}^n - N_{J,k}^n \} & (M_{J,k}^n < 0) \end{cases} \tag{36a}$$

$$I_{22}\begin{cases} =f(x,y)N^{n}_{j,k}\{N^{n}_{j,k}-N^{n}_{j,k-1}\} & (N^{n}_{j,k}\geq 0) \\ =f(x,y)N^{n}_{j,k}\{N^{n}_{j,k+1}-N^{n}_{j,k}\} & (N^{n}_{j,k}<0) \end{cases} \tag{36b}$$

$$\zeta^{n+3}_{j,k}=\zeta^{n+1}_{j,k}-\Theta\{M^{n+2}_{j+1,k}-M^{n+2}_{j-1,k}+N^{n+2}_{j,k+1}-N^{n+2}_{j,k-1}\} \tag{37}$$

At the opening point (m, n), the value $N_{m,n}(=V_{m,n}(h+\zeta))$ is replaced by $N^{*}_{m,n}$, denoting an opening width by ℓ

$$N^{*}_{m,n}=\frac{\ell}{2\Delta s}N_{m,n}\ . \tag{38}$$

Coefficients in the above equations are given below,

$$a(x,y)=g(h+\zeta)\Delta t/\Delta s \qquad b=4\omega(\sin\varphi)\Delta t=2f\Delta t$$
$$c=2\Delta t/\rho_w \qquad d(x,y)=\gamma_b^2\rho_w/(h+\zeta)^2$$
$$e=\Delta t/\Delta s \qquad f(x,y)=2\Delta t/(h+\zeta)\Delta s$$

where $a(x,y)$, $d(x,y)$ and $f(x,y)$ may be computed every n-th time-step (in our case every 20 min = $40\Delta t$), because they vary very slowly.

The variables thus computed must be smoothed by adding a certain proportion of the mean value computed from the four surrounding points after completion of n-th time-step, to obtain a probale value, e.g.

$$(M^{n}_{j,k})=\alpha M^{n}_{j,k}+\frac{1-\alpha}{4}(M^{n}_{j+1,k}+M^{n}_{j-1,k}+M^{n}_{j,k+1}+M^{n}_{j,k+1}) \tag{39}$$
$$(0\leq\alpha\leq 1)$$

For economy of the computation time, the discharge fluxes, M and N have been calculated every odd time step, and the elevation ζ every even time step. Likewise, the grid points for M, N and ζ were arranged alternatively, i.e. the values of M and N were determined on grid points where water depths are assigned in Fig. 1, the values of ζ on grid points where depths are not written.

CONNECTION OF SUBREGIONS

In our study of the Typhoon tide prediction, the numerical integration region was inevitably divided into two regions (Fig. 1). Because the water depths differ greatly between the inside and the outside of the entrance of the bay, the stability condition for grid dimensions, eq. (9), requires entirely different grid width for each of the two regions. In such a case, usual prediction precedures are too much cumbersome. Firstly, a rough calculation is made either for both regions with the same rough grid as the outer or only for the outer region neglecting the smaller one, to obtain the change of the water level at the entrance of the bay-the boundary condition for the second calculation. Using the values of ζ at the entrance thus determined as input data, the second precise computation may be carried out for the very interested region with finer grid width.

In order to complete the calculation by one procedure, the two regions are to be overlapped at the neck of the bay. Grid points B, C, D and E in Fig. 2 stand in common for both regions. (In Fig. 2, circles show points for M and N, crosses for ζ). The values of M and N at D as

a grid point of the outer subregion are decided as mean values at points on X - Y determined by calculation in the inner subregion On the other hand, the values of ζ on B - C to be used as boundary condition for the inner are chosen equal to that at E determined from the outer region. The values of ζ on X" - Y" may be obtained from values of M and N in the inner region one time-step before. Thus, ζ on X' - Y' may be determined as mean of four surrounding points on B - C and X" - Y".

NUMERICAL CALCULATION

MODEL OF TYPHOON

Before a series of detailed numerical calculations, reliability of prediction procedures was checked by comparison of a record of an observed surge (caused by Typhoon No 5821) with calculation. Considerably good agreement between them was confirmed. (Fig. 3 is an example of comparisons.)

A model of typhoon was chosen as that which caused the severest damages ever experienced in Japan, named the Ise-Bay Typhoon. The typhoon was assumed to proceed northwards along the course parallel to axis of the bay about 40 km west of Tokyo with speed of 73 km/hr (A-course in Fig. 4). Subsidarily, two other courses (named E- and I-course) were also investigated. In the earlier study, several courses parallel to them were compared to decide the worst ones. Course A coincides with that of a typhoon (attacked on Oct. 1, 1917) which caused the severest damages on coast of the ba

Constants used in this study are as follows:

Typhoon : $a = 7 \times 10^4$ (dyne/cm^2), $a/\rho_w g = 71.5$ (cm), $r_0 = 7.5 \times 10^6$ (cm), $\zeta_o = 1.028 \times 10^3$ (cm), $V = 2.02 \times 10^3$ (cm/sec) (speed of Typhoon), $\rho_a = 1.293 \times 10^{-3}$ (gr/cm^3), $C_1 \approx 4/7$, $C_2 \approx 0.6$

Grid : $\Delta s = 1.5 \times 10^5$ (cm) (for the inner region) and 6×10^5 (cm) (for the outer region), $\Delta t = 30$ (sec),

External faces : $\gamma^2 \rho_a = 3.2 \times 10^{-6}$ (gr/cm^3), $\gamma_b^2 \rho_w = 2.6 \times 10^{-3}$, $k = 0.5$.

EFFECT OF DIKE ON REDUCTION OF SURGES

The opening of the dike should preferablly be wide from the standpoint of navigation. On the other hand, the effects of the dike on the reduction of surges will be increased with decrease in the opening width. Here, we must determine the most preferable opening width to suffice both requirements.

A series of computations has been carried out for different opening widths, i.e. for a) the present state (no dike), for the central opening with length b) 2000 m, c) 1000 m, d) 1000 m (with shallow opening depth: Hop = 21 m) and e) 500 m and for f) two openings each 500 m at both ends of the dike.

In these calculations, the Coriolis force and the quadratic type of bottom friction are considered at every grid point. However, the inertial term is considered only at the opening where it becomes exceedingly predominant. An alternative of the inertial-term method is to make use of discharge coefficient due to contraction ($V_{m,n} = \pm K\sqrt{2g\,|\zeta_{m,n+1} - \zeta_{m,n-1}|}$) Both the methods have been shown to give the same results [Unoki and Isozaki (1962)] . Fig. 5 shows comprehensively results of computations for the course A, illustrating the reduction of maximum surge elevation with decreasing opening width. The time variations of elevations with

progress of the typhoon are given in Fig. 6. Fig. 7 is graphs of contour lines (in cm) every one hour. A peak water level at Chiba occurs at 8 h 20 m.

Figs. 8 and 9 give results for the courses E and I respectively.

For typhoons along the course-A, empirical relations, eq. (40), between the maximum water level inside the dike and the opening area have been obtained as shown in Fig. 10,

$$\zeta_{max} = a + m \log A \quad (1.3 \times 10^4 \ m^2 \leq A \leq 5.5 \times 10^4 \ m^2) . \qquad (40)$$

where A means the cross sectional area of opening, a constant m is almost independent of the position of observation,while a in eq. (40) is a constant dependent on position. The location of openings has almost no direct influence on the effect of the dike. It should be noticed that there results no appreciable increase in peak water level in the outside of the dike. In some cases, the maximum water levels in the outside rather decrease slightly.

DAILY TIDE AND DISCHARGE VELOCITY AT THE OPENING

Numerical calculation of the astronomical tide (the semi-diurnal M_2 tide) for the present state has been compared with the estimated in Fig. 11, showing a remarkably good agreement between them. In order to protect the dike from erosion and to secure the safety of navigation, the maximum discharge velocity at the opening should not exceed some limit.

A model of spring tide which is composed of 13 components has been assumed to estimate the maximum discharge velocity. It amounts to 1.9 m/sec and 2.0 m/sec for opening (length 1000 m) with depths of 28 m and 21 m, respectively. (Fig. 12)

INTERACTION BETWEEN DAILY TIDE AND TYPHOON TIDE

As far as the above treatments are concerned, we considered only the water level rise due to tropical cyclones In practice, the catastrophic damages have been experienced when peak storm surges superposed on high tidal level. Superposition of both phenomena may be allowed in the cases where effects of non-linear terms are negligible. However, in our study of the dike across the Bay, the inertial terms govern so strictly the liquid motion that we can no more admit the superposition.

Because the motivation of tidal motion is given at the boundary of integration region, the stationary movement of tide can be attained after about 36 hours from the beginning (Fig. 11). As a consequence, it needs very long computation time to obtain exact solutions of the problem of superposition.

Figs. 13 and 14 are supplied to demonstrate that the superposition of daily tide and typhoon tide overestimates surge elevations. In these computations, the peak of storm surge is chosen to occur just at high tidal level.

The amounts of reduction in maximum surge elevation within the dike are far increased as a result of interaction. Thus, the construction of dike is extremely effective.

For the outside of the dike, superposition may be admitted.

Maximum velocity at the opening is given to be 3.25 m/sec (width 1000 m, depth 28 m). (Fig. 12b)

EFFECT OF TYPHOON SPEED AND WIND STRESS

Storm surges are affected by a number of factors. Of course, topography is a governing factor. It is a point of practical interest how speed of storm affects the water level rise. In the case of Tokyo Bay, the point has been thoroughly investigated by S. Unoki and I. Isozaki (1962). They concluded from a series of numerical calculations that the speed of Typhoon has no significant effect within the range of speed from 40 km/h to 80 km/h. This is surprising because the average velocity of long waves propagating the bay is about 55 - 60 km/h. There exist no resonance phenomenon in the region limited by a boundary.

Relative contribution of the atmospheric pressure drop and the wind stress is also an interesting problem. Numerical experiments by us for Tokyo Bay (without the dike, the typhoon model A) show that both have the same order of effects (Fig. 15). Of course, in the outer part the effect of atmospheric pressure drop is far predominant over the wind stress (see the curve for Kurihama).

Acknowledgement

The authors are greatly indebted to Dr. S. Unoki, Meteorological Research Institute of Japan, for his valuable advice.

REFERENCES

Ito, T., Watanabe, J., Hino, K. and Hino, M. (1963): Some remarks on numerical prediction of typhoon tide, Proc. 8th Conference on Hydraulic Research, Japan, Japan Soc. Civil Eng.

Ito, T., Hino, M. and Hino, K. (1964): Summary report: Numerical calculations on the effects of the dike across Tokyo Bay on reduction of typhoon tides, Report No.300, Sangyo Keikaku Kaigi (Council for Industry Planning).

Jansen, P. Ph. and Dronkers, J.J. (1962): Memorandum on dike construction as a part of a masterplan for Tokyo Bay. Sangyo Keikaku Kaigi (Council for Industry Planning)

Miyazaki, M. (1961): Chapters 4, 5 and 6 in "Numerical calculations of typhoon tide and counter plans as a part of Neo Tokyo Plan", Sangyo Keikaku Kaigi (Council for Industry Planning).

Sangyo Keikaku Kaigi (Council for Industry Planning) (1961): Recommendations on construction of a dike across Tokyo Bay as a resolution of typhoon tide and traffic problems.

Shuman, F.G. (1962): Numerical experiments with primitive equations. Proc. International Symposium on Numerical Weather Prediction in Tokyo, Nov. 7-13, 1960.

Unoki, S. and Isozaki, I. (1962a): On some results of numerical experiments on typhoon tide. Proc. of 9th Conference on Coastal Engineering, Japan, Japan Soc. Civil Eng.

Unoki, S. and Isozaki, I. (1962b): Comment on numerical calculation of velocity at an opening of dike, ibid. A translated text of the above two papers entitled "On the effect of a dike with openings on the storm surge caused by a typhoon" is collected in Coastal Engineering in Japan, VI (1963).

Welander, P. (1961): Numerical prediction of storm surges.
Advances in Geophysics, vol. 8, Academic Press.

CAPTIONS

Fig. 1. The grid points used in the calculation. Numbers on mesh point mean water depth where discharge fluxes are determined

Fig. 2. Overlapping of two regions. Circles represent grid points where discharge fluxes are to be determined, while crosses correspond to points for water level.

Fig. 3. An example of comparison between observed and calculated storm surges.

Fig. 4. Three typical courses of typhoon. Numbered circles show position of typhoon center every one hour.

Fig. 5. Summary representation of calculated maximum surge elevations on the coast caused by the hypothetical Ise-Bay Typhoon along the A-course.

Fig. 6. Predictions of water levels at various point on coast of Tokyo Bay, showing effects of the dike opening on the reduction of surges

Fig. 7. Contour lines of sea level elevations (in cm) by the Ise-Bay Typhoon along course-A.

Fig. 8. Maximum surge elevations at various points caused by the Ise-Bay Typhoon along course-E.

Fig. 9. Maximum surge elevations caused by the Ise-Bay Typhoon along course-I.

Fig. 10. Empirical relationships between maximum surge elevations at points within the inner part of the dike and the cross sectional area of opening.

Fig. 11. Comparisons of the calculated semi-diurnal M_2 tide with the estimated (at Tokyo and Yokohama).

Fig. 12. Tidal velocity at the opening (calculated results).

Fig. 13. Predictions of water levels at various points, when storm surge occurs at high tidal level.

Fig. 14. Summary representation of maximum surge elevation when surge superposes on high tidal level. Linear superposition of daily tide and storm surge overestimates the maximum when the proposed dike is constructed.

Fig. 15. Relative contribution of atmospheric pressure drop and wind stress. The solid lines represent total effect, the dashed lines the atmospheric pressure effect. The calculation has been made for present state (no dike) with the hypothetical Ise-Bay-Typhoon along course-A.

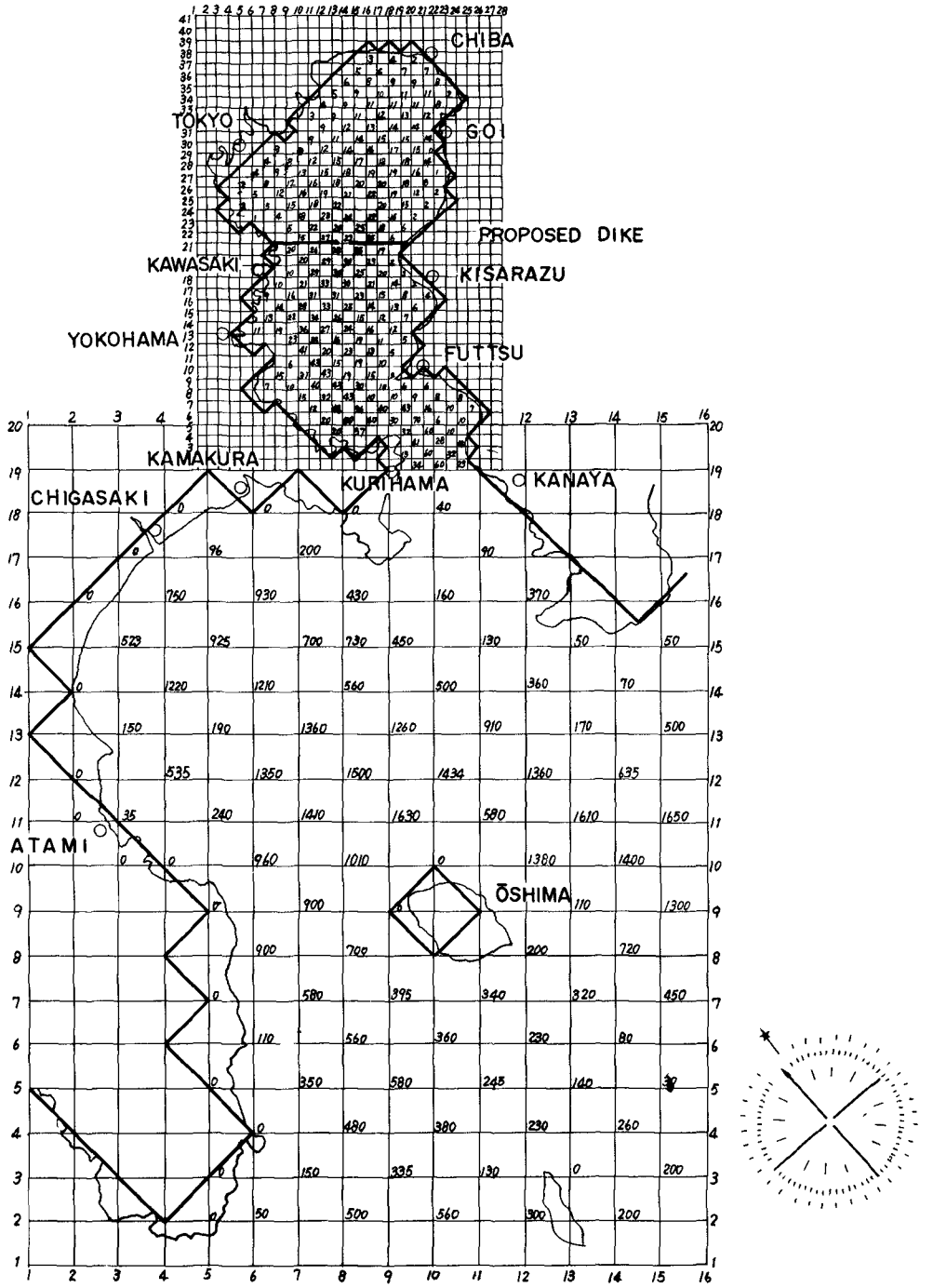
CHIBA
TOKYO
GOI
PROPOSED DIKE
KAWASAKI
KISARAZU
YOKOHAMA
FUTTSU
KAMAKURA
KURIHAMA
KANAYA
CHIGASAKI
ATAMI
ŌSHIMA

FIG - 1

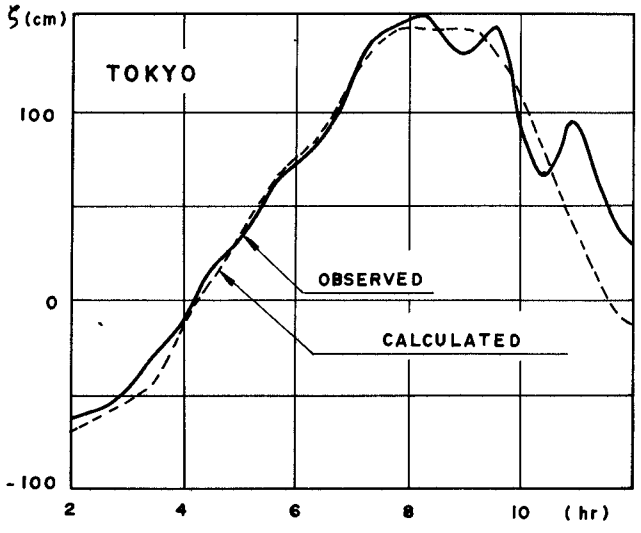
ζ (cm)
TOKYO
100
0
-100
OBSERVED
CALCULATED
2
4
6
8
10
(hr)

FIG - 2

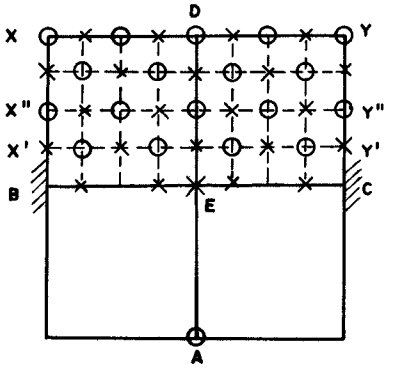
D
X
Y
X"
Y"
X'
Y'
B
C
E
A

FIG - 3

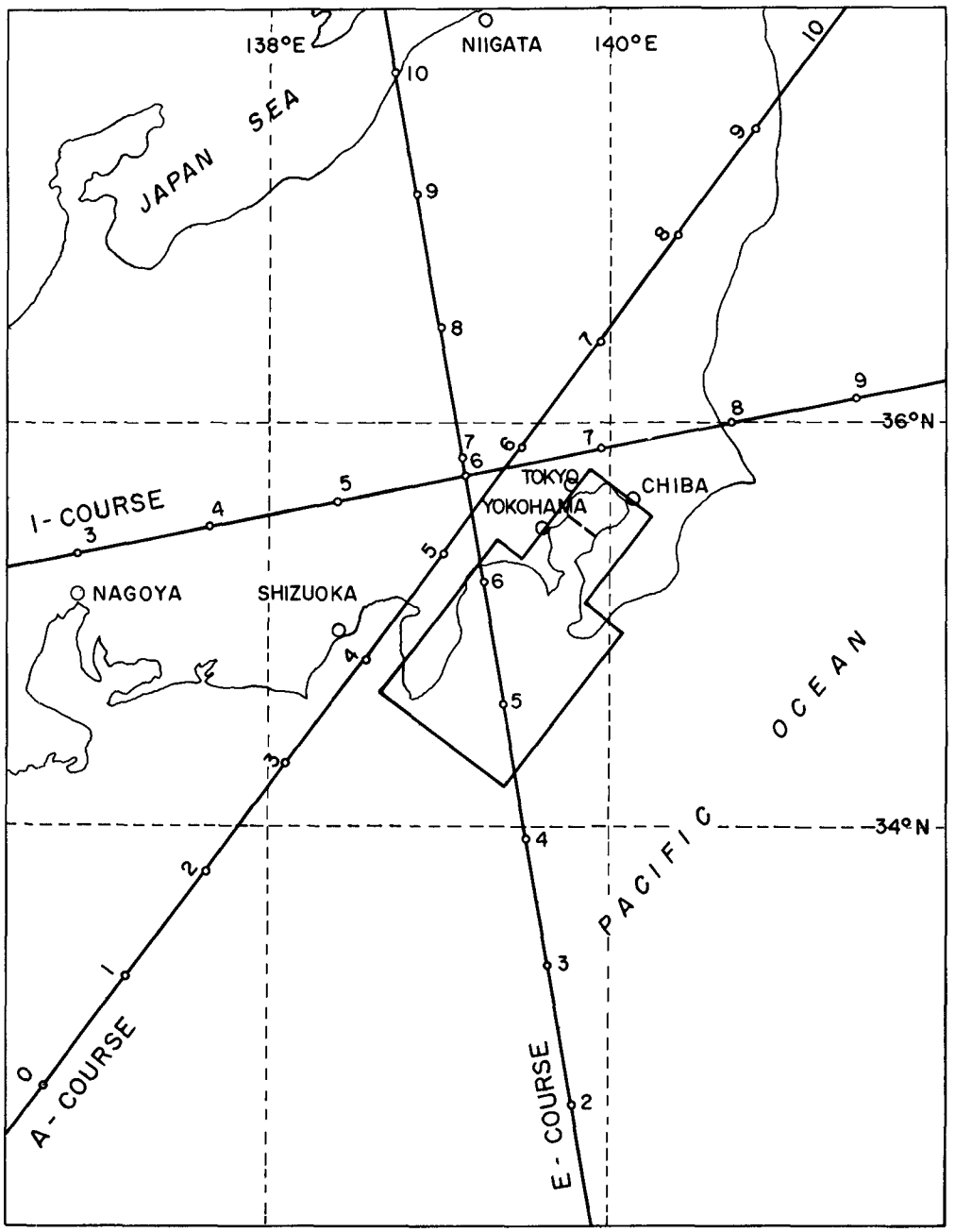
138°E
NIIGATA
140°E
JAPAN SEA
36°N
34°N
I-COURSE
A-COURSE
E-COURSE
TOKYO
YOKOHAMA
CHIBA
NAGOYA
SHIZUOKA
PACIFIC OCEAN

FIG - 4

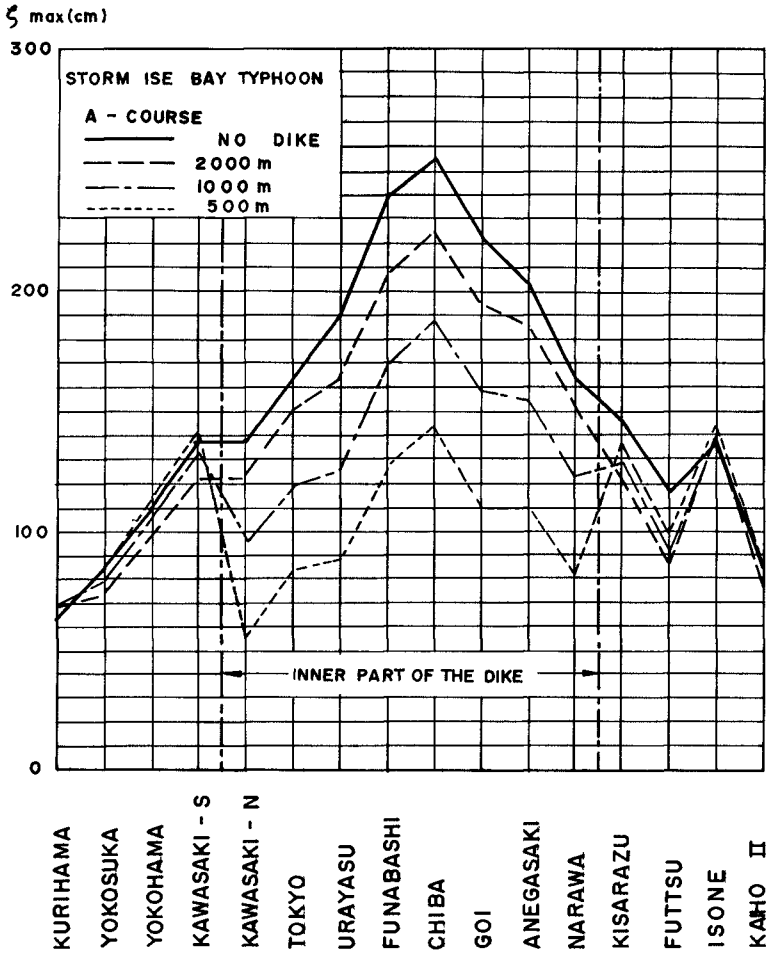
ζ max(cm)
300
200
100
0
STORM ISE BAY TYPHOON
A - COURSE
NO DIKE
2000 m
1000 m
500 m
INNER PART OF THE DIKE
KURIHAMA
YOKOSUKA
YOKOHAMA
KAWASAKI - S
KAWASAKI - N
TOKYO
URAYASU
FUNABASHI
CHIBA
GOI
ANEGASAKI
NARAWA
KISARAZU
FUTTSU
ISONE
KAHO II

FIG - 5

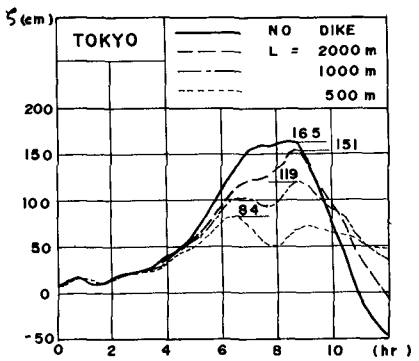
TOKYO
NO DIKE
L = 2000 m
1000 m
500 m
165
151
119
84
ζ(cm)
(hr)

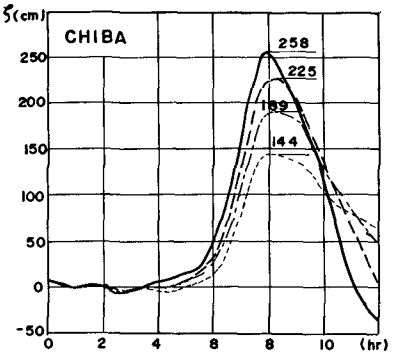
CHIBA
258
225
192
144
ζ(cm)
(hr)

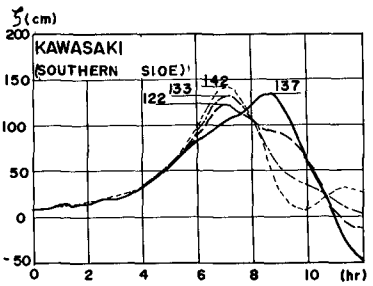
KAWASAKI
(SOUTHERN SIDE)
142
133
122
137
ζ(cm)
(hr)

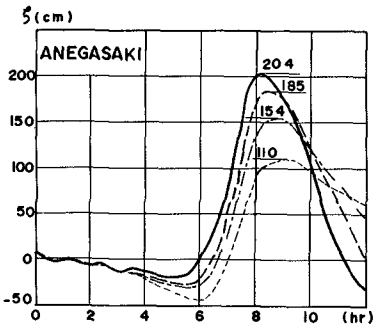
ANEGASAKI
204
185
154
110
ζ(cm)
(hr)

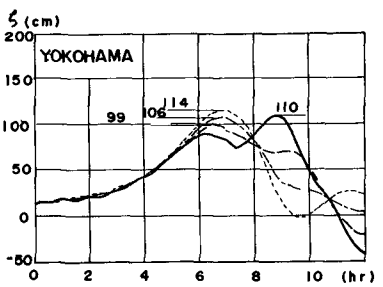
YOKOHAMA
99
106
114
110
ζ(cm)
(hr)

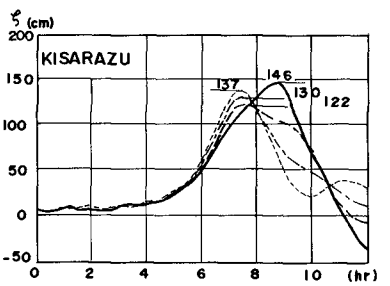
KISARAZU
137
146
130
122
ζ(cm)
(hr)

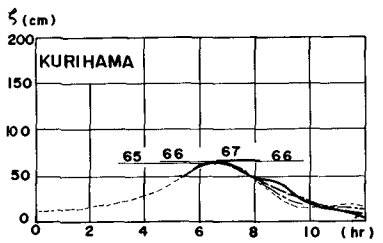
KURIHAMA
65
66
67
66
ζ(cm)
(hr)

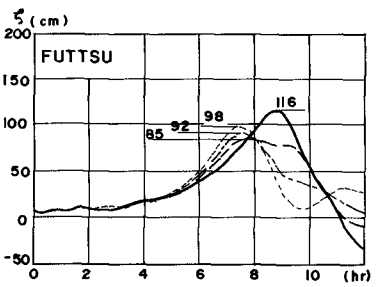
FUTTSU
85
92
98
116
ζ(cm)
(hr)

FIG - 6

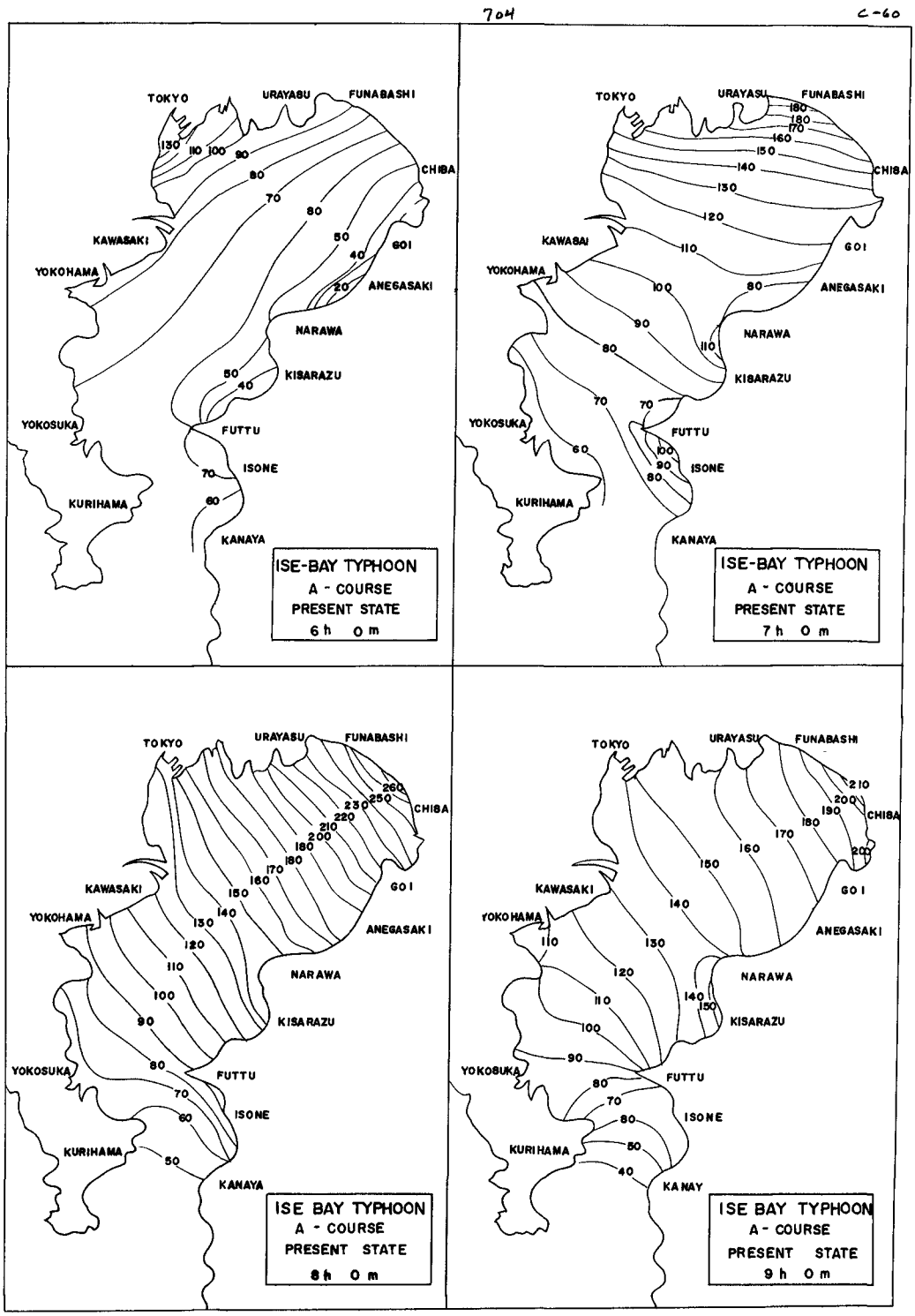
704
C-60
TOKYO
URAYASU
FUNABASHI
CHIBA
KAWASAKI
YOKOHAMA
GOI
ANEGASAKI
NARAWA
KISARAZU
YOKOSUKA
FUTTU
ISONE
KURIHAMA
KANAYA
ISE-BAY TYPHOON
A - COURSE
PRESENT STATE
6 h 0 m
ISE-BAY TYPHOON
A - COURSE
PRESENT STATE
7 h 0 m
ISE BAY TYPHOON
A - COURSE
PRESENT STATE
8 h 0 m
ISE BAY TYPHOON
A - COURSE
PRESENT STATE
9 h 0 m

FIG 7 (a)

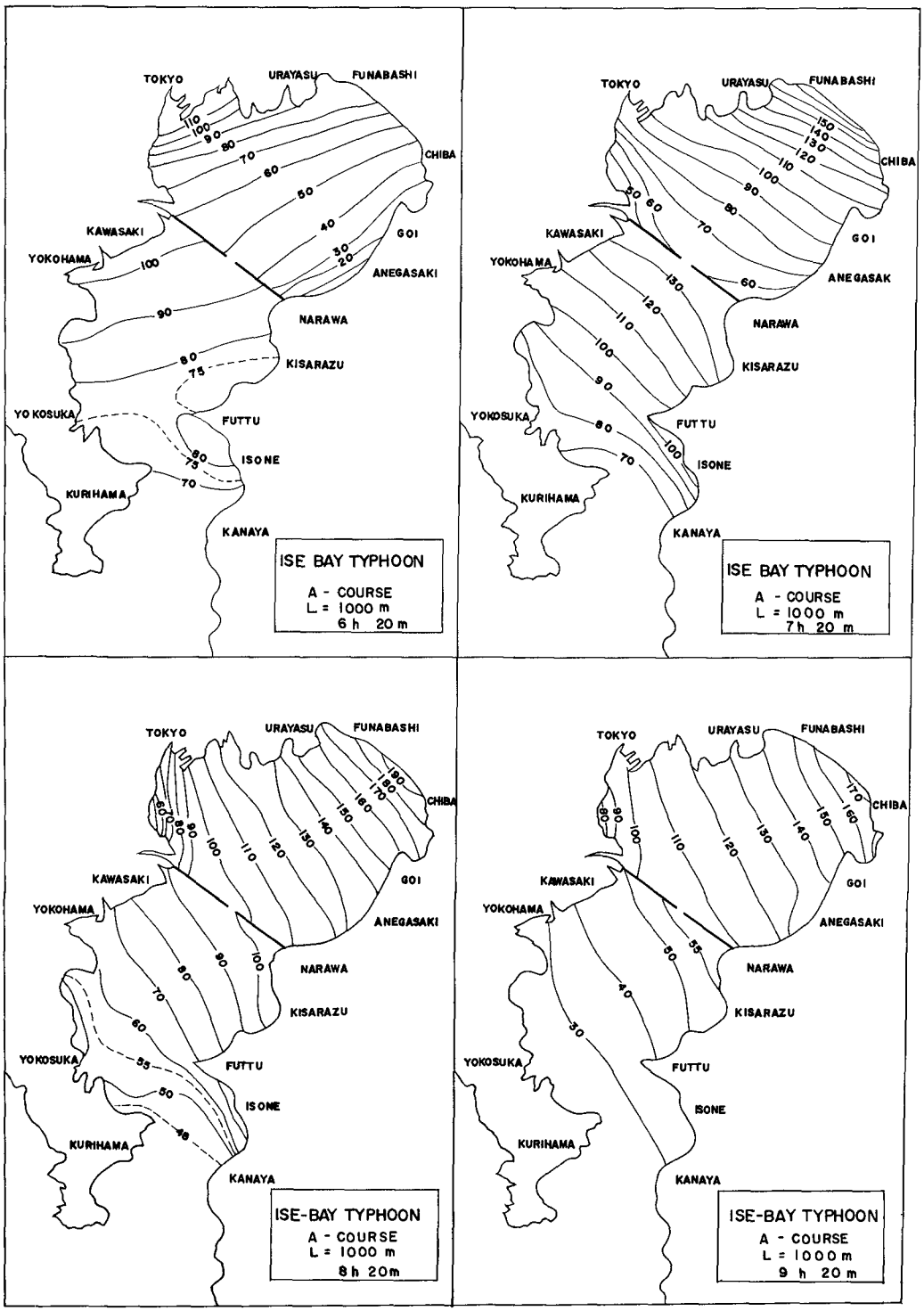
TOKYO
URAYASU
FUNABASHI
CHIBA
GOI
ANEGASAKI
NARAWA
KISARAZU
FUTTU
ISONE
KANAYA
KURIHAMA
YOKOSUKA
KAWASAKI
YOKOHAMA
ISE BAY TYPHOON
A - COURSE
L = 1000 m
6 h 20 m
ISE BAY TYPHOON
A - COURSE
L = 1000 m
7h 20 m
ISE-BAY TYPHOON
A - COURSE
L = 1000 m
8h 20m
ISE-BAY TYPHOON
A - COURSE
L = 1000 m
9 h 20 m

FIG - 7 (b)

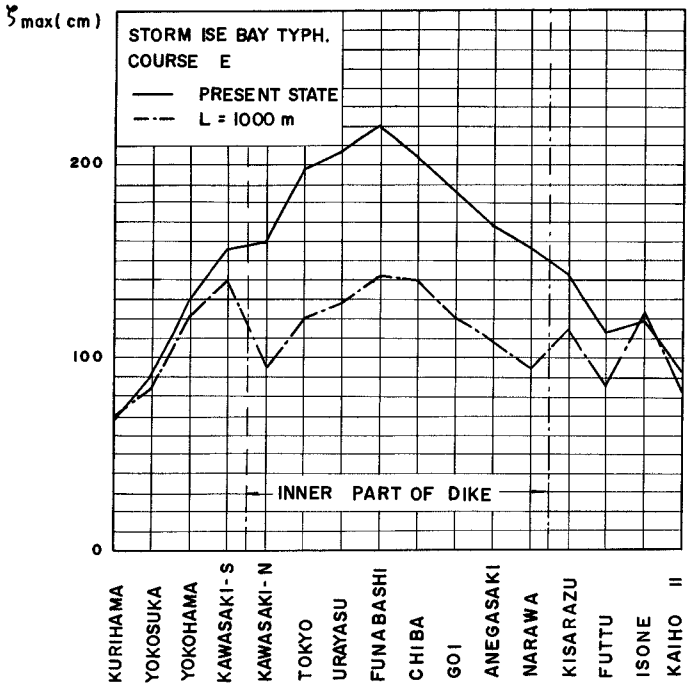
ζmax(cm)
STORM ISE BAY TYPH.
COURSE E
PRESENT STATE
L = 1000 m
200
100
0
INNER PART OF DIKE
KURIHAMA
YOKOSUKA
YOKOHAMA
KAWASAKI-S
KAWASAKI-N
TOKYO
URAYASU
FUNABASHI
CHIBA
GOI
ANEGASAKI
NARAWA
KISARAZU
FUTTU
ISONE
KAIHO II

FIG 8

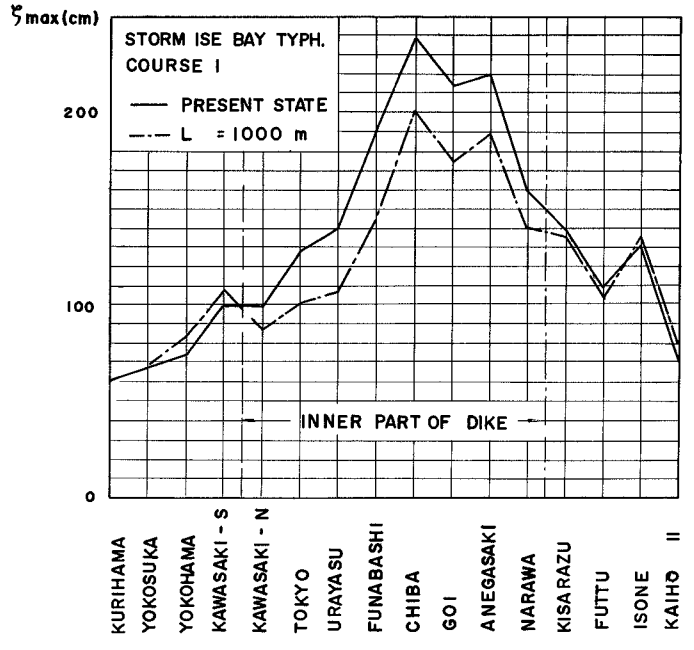
ζmax(cm)
STORM ISE BAY TYPH.
COURSE I
PRESENT STATE
L = 1000 m
200
100
0
INNER PART OF DIKE
KURIHAMA
YOKOSUKA
YOKOHAMA
KAWASAKI-S
KAWASAKI-N
TOKYO
URAYASU
FUNABASHI
CHIBA
GOI
ANEGASAKI
NARAWA
KISARAZU
FUTTU
ISONE
KAIHO II

FIG 9

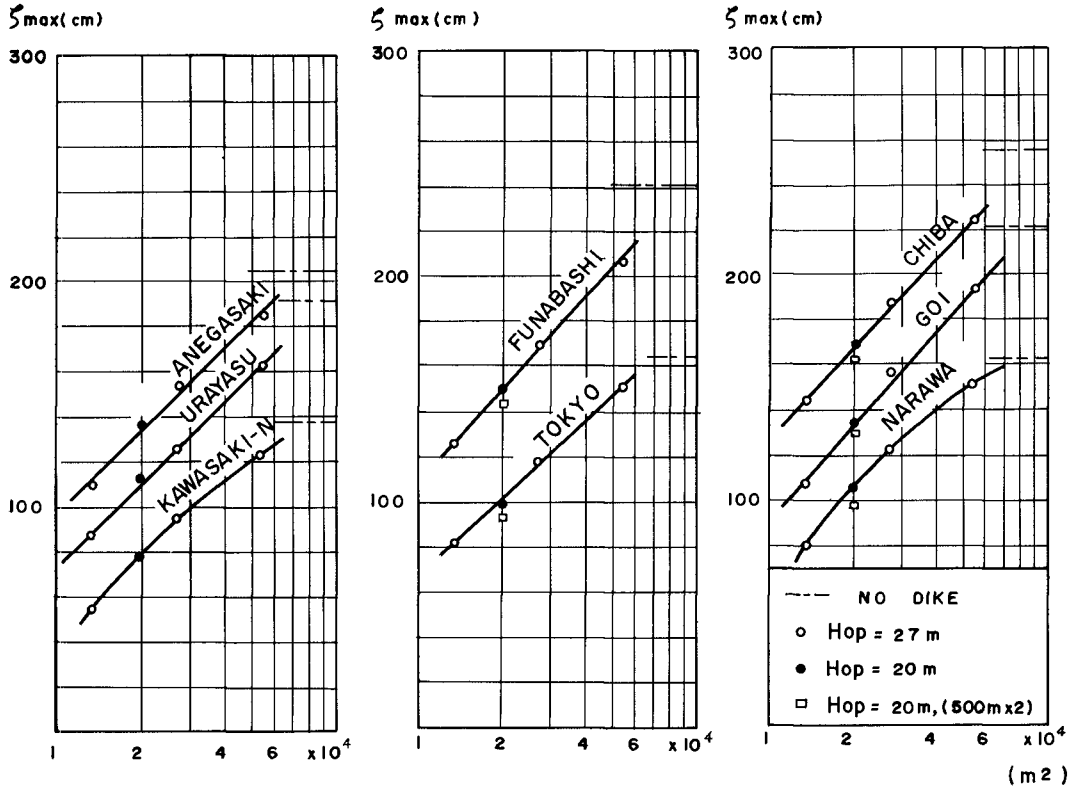
ζmax(cm)
300
200
100
ANEGASAKI
URAYASU
KAWASAKI-N
1
2
4
6
x10⁴
ζ max(cm)
FUNABASHI
TOKYO
CHIBA
GOI
NARAWA
NO DIKE
Hop = 27 m
Hop = 20 m
Hop = 20m,(500mx2)
(m2)

FIG - 10

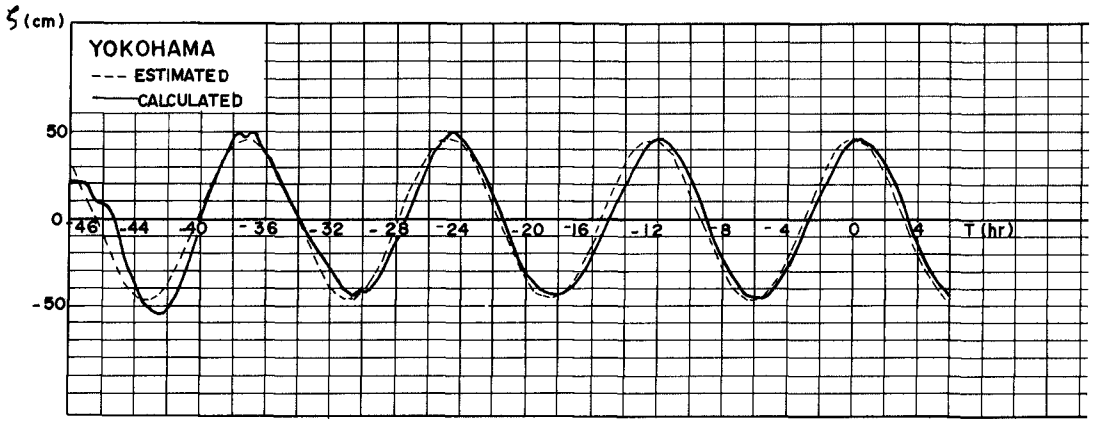
ζ (cm)
YOKOHAMA
--- ESTIMATED
——CALCULATED
50
0
-50
-46
-44
-40
-36
-32
-28
-24
-20
-16
-12
-8
-4
0
4
T (hr)

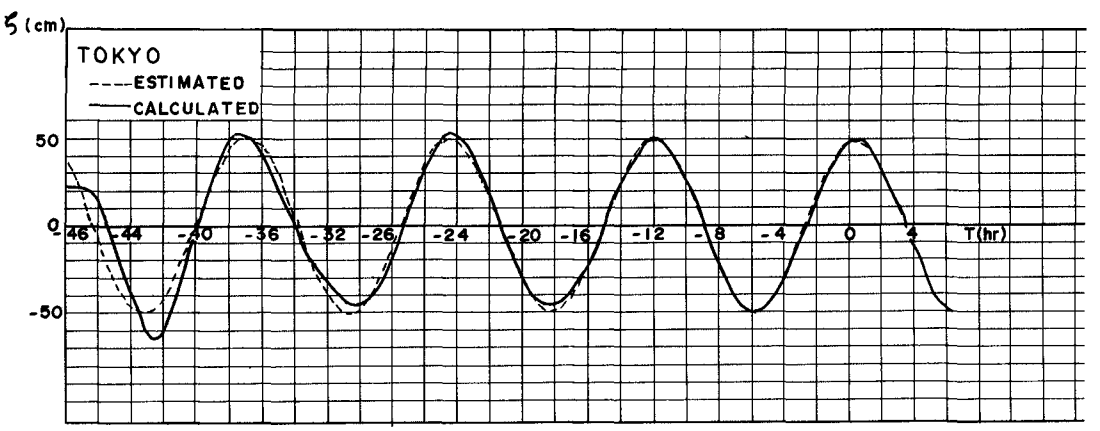
ζ (cm)
TOKYO
----ESTIMATED
——CALCULATED
50
0
-50
-46
-44
-40
-36
-32
-26
-24
-20
-16
-12
-8
-4
0
4
T(hr)

FIG - 11

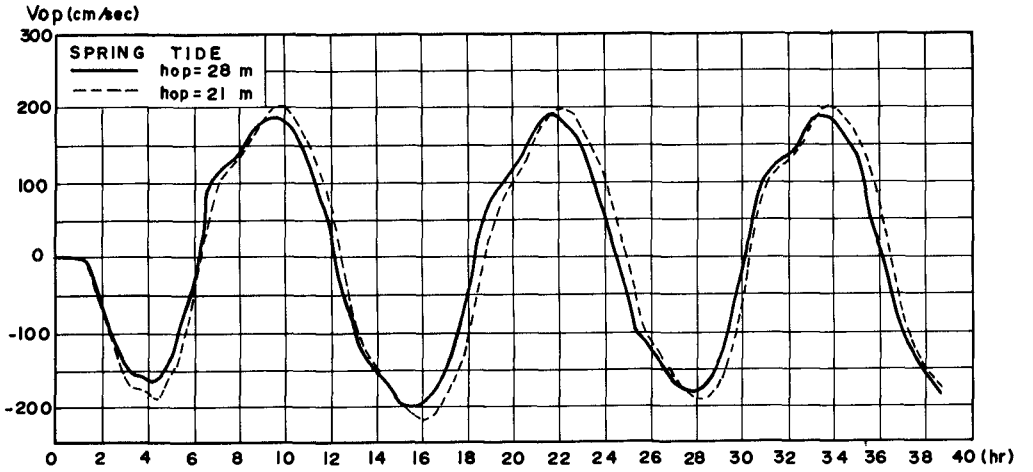
Vop (cm/sec)
SPRING TIDE
hop = 28 m
hop = 21 m
300
200
100
0
-100
-200
0 2 4 6 8 10 12 14 16 18 20 22 24 26 28 30 32 34 36 38 40 (hr)

(a)

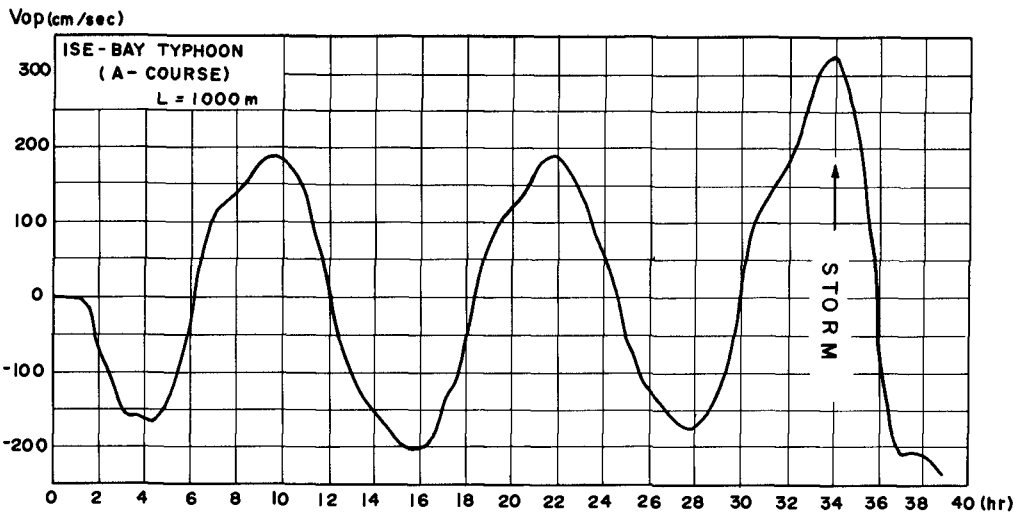
Vop (cm/sec)
ISE-BAY TYPHOON
(A-COURSE)
L = 1000 m
300
200
100
0
-100
-200
STORM
0 2 4 6 8 10 12 14 16 18 20 22 24 26 28 30 32 34 36 38 40 (hr)

(b)

FIG - 12

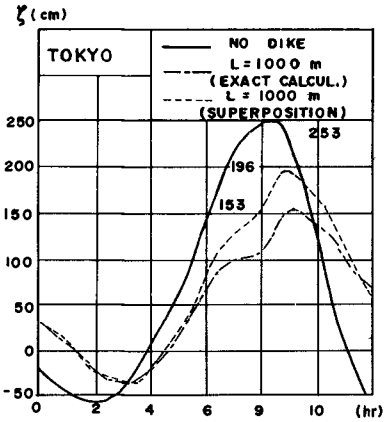
ζ (cm)
TOKYO
NO DIKE
L=1000 m
(EXACT CALCUL.)
L = 1000 m
(SUPERPOSITION)
253
196
153
(hr)

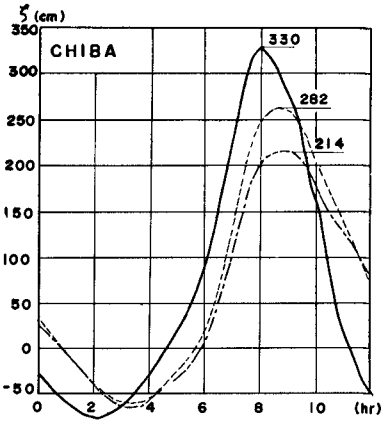
ζ (cm)
CHIBA
330
282
214
(hr)

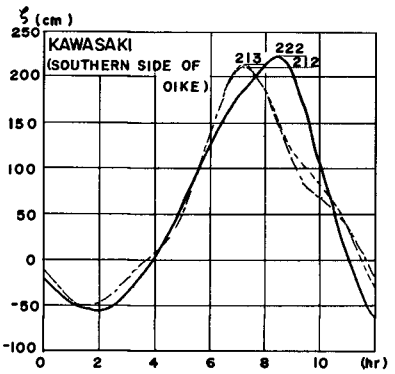
ζ (cm)
KAWASAKI
(SOUTHERN SIDE OF DIKE)
213
222
212
(hr)

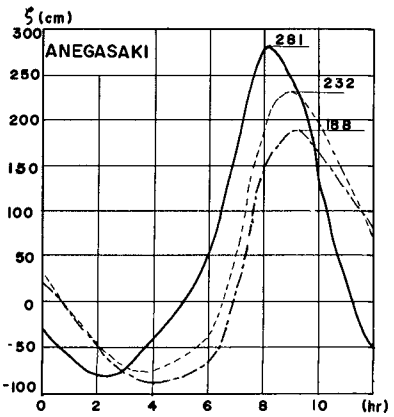
ζ (cm)
ANEGASAKI
281
232
188
(hr)

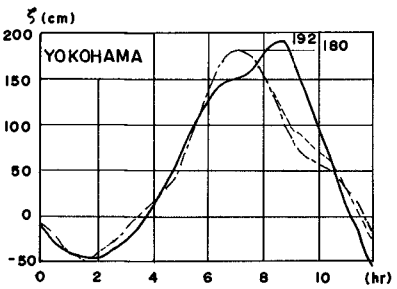
ζ (cm)
YOKOHAMA
192
180
(hr)

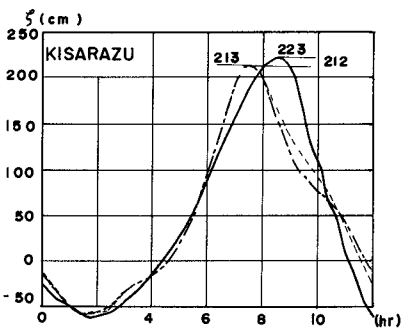
ζ (cm)
KISARAZU
213
223
212
(hr)

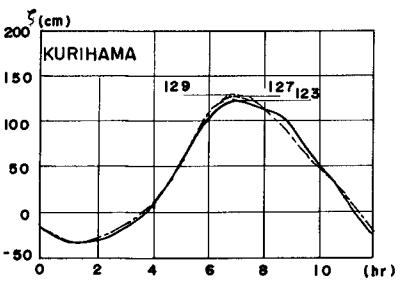
ζ (cm)
KURIHAMA
129
127
123
(hr)

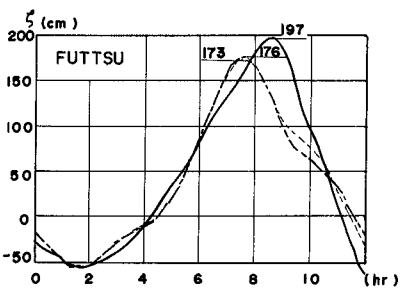
ζ (cm)
FUTTSU
197
173
176
(hr)

FIG - 13

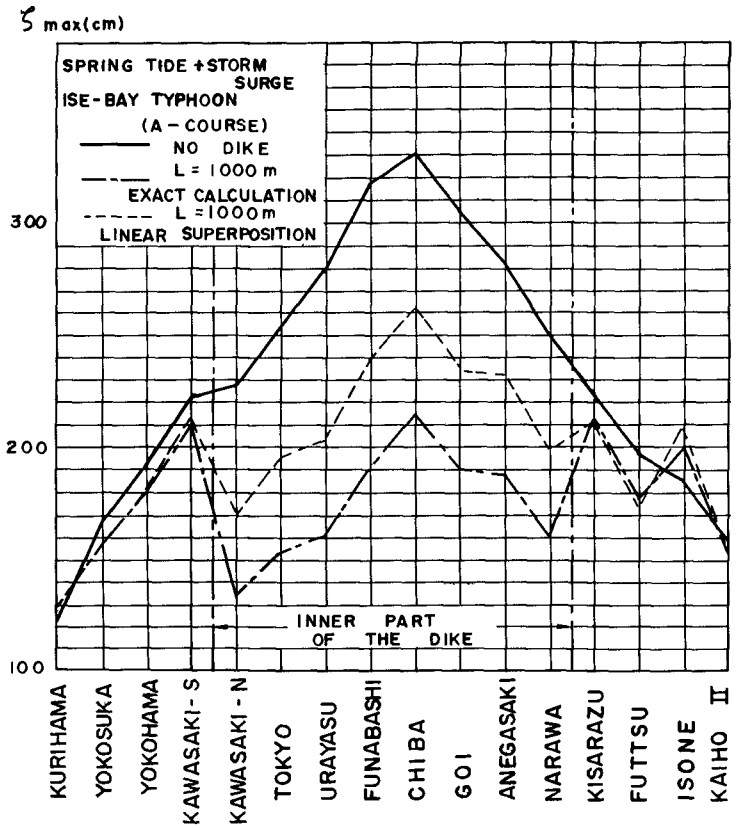
ζ max(cm)
SPRING TIDE + STORM SURGE
ISE-BAY TYPHOON
(A-COURSE)
NO DIKE
L = 1000 m
EXACT CALCULATION
L = 1000 m
LINEAR SUPERPOSITION
300
200
100
INNER PART OF THE DIKE
KURIHAMA
YOKOSUKA
YOKOHAMA
KAWASAKI-S
KAWASAKI-N
TOKYO
URAYASU
FUNABASHI
CHIBA
GOI
ANEGASAKI
NARAWA
KISARAZU
FUTTSU
ISONE
KAIHO II

FIG-14

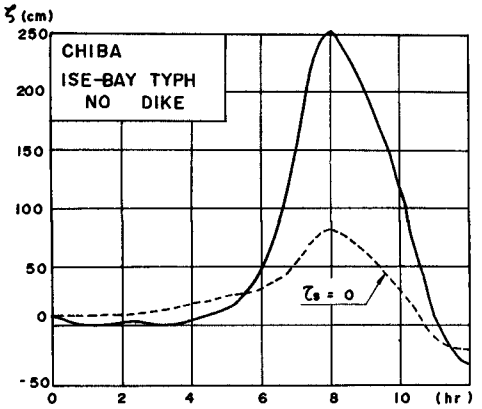
ζ (cm)
250
200
150
100
50
0
-50
CHIBA
ISE-BAY TYPH
NO DIKE
τs = 0
0
2
4
6
8
10
(hr)

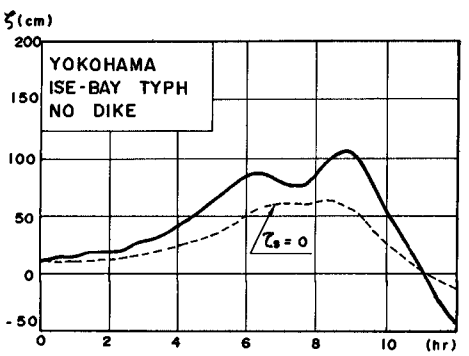
ζ (cm)
200
150
100
50
0
-50
YOKOHAMA
ISE-BAY TYPH
NO DIKE
τs = 0
0
2
4
6
8
10
(hr)

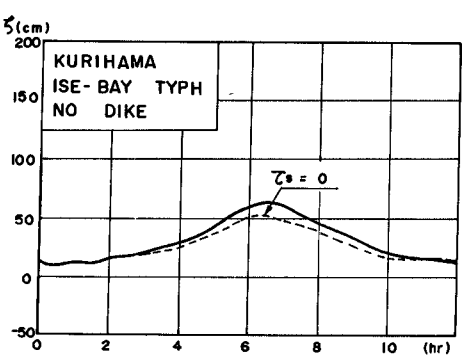
ζ (cm)
200
150
100
50
0
-50
KURIHAMA
ISE-BAY TYPH
NO DIKE
τs = 0
0
2
4
6
8
10
(hr)

FIG - 15